Acta Oceanol. Sin., 2025, Vol. 44, No. 1, P. 28–35
https://doi.org/10.1007/s13131-024-2443-3

The role of Luzon Strait transport in shallow meridional overturning circulation of South China Sea

Kun Jiang[1, 2], Yu Wang[3*], Yan Sun[1, 2], Jian Lan[1, 2, 4]

[1] Frontiers Science Center for Deep Ocean Multispheres and Earth System and Physical Oceanography Laboratory, Ocean University of China, Qingdao 266100, China

[2] College of Oceanic and Atmospheric Sciences, Ocean University of China, Qingdao 266100, China

[3] National Marine Environmental Monitoring Center, Dalian 116023, China

[4] Laoshan Laboratory, Qingdao 266237, China

Received 9 July 2024; accepted 11 November 2024

Abstract

The impacts of the Luzon Strait transport on shallow meridional overturning circulation (SMOC) in the South China Sea (SCS) have been pointed out by previous studies, but the issue whether the Luzon Strait transport dominates the SMOC formation still remains open. The Helmholtz decomposition is applied based on the ocean general circulation model for the earth simulator products to address this issue. Results show that the motion caused by the Luzon Strait transport is characterized as an obvious southward flow between 13°N and 20°N. After this motion being removed, the clockwise winter SMOC and the anticlockwise summer SMOC can still exist significantly. The SMOC existence and its seasonal variation are also reproduced in the numerical simulation with the Luzon Strait closed. Both results of the Helmholtz decomposition and numerical experiment suggest that the SMOC formation and its seasonal variation are not dominated by the Luzon Strait transport. The SCS monsoon is the primary driving factor for the SMOC, which is related to the physical processes within the SCS.

Key words South China Sea, Luzon Strait transport, shallow meridional overturning circulation, Helmholtz decomposition

Citation Jiang Kun, Wang Yu, Sun Yan, Lan Jian. 2025. The role of Luzon Strait transport in shallow meridional overturning circulation of South China Sea. Acta Oceanologica Sinica, 44(1): 28–35, doi: 10.1007/s13131-024-2443-3

1 Introduction

The South China Sea (SCS) is a semi-enclosed marginal sea of the North Pacific Ocean. It extends from the equator to 23°N and from 99°E to 121°E, with an average water depth of over 2 000 m and the maximum depth of approximately 4 700 m (Chu and Li, 2000). The SCS connects the adjacent seas through the Taiwan, Luzon, Mindoro, Balabac, Karimata and Malacca Straits. The Luzon Strait is the only deep strait with a sill depth of about 2 400 m, and it plays a major role in the water exchange between the SCS and the Pacific Ocean (Qu et al., 2006; Deng et al., 2018; Wu et al., 2021).

The annual mean Luzon Strait transport is westward, with transport ranging from 2×10^6 m^3/s to 10×10^6 m^3/s (Metzger and Hurlburt, 1996; Xue et al., 2004; Fang et al., 2005, 2009; Yaremchuk et al., 2009; Hsin et al., 2012). Its sandwiched vertical structure has been proposed based on historical oxygen data and current observations (Qu, 2002; Tian et al., 2006). Through the Luzon Strait, water flows into the SCS in the upper and deep layers but flows out of the SCS in the intermediate layer. The Luzon Strait transport has a distinct seasonal variation, with stronger transport in winter and weaker transport in summer (Qu, 2000; Fang et al., 2005; Yaremchuk et al., 2009; Zhang et al., 2015). This seasonal variation is attributed to the seasonal reversal of the SCS monsoon (Metzger and Hurlburt, 1996; Zhao et al., 2009; Hsin et al., 2012), as well as the influence of the Kuroshio transport east of Luzon (Qu et al., 2004; Yaremchuk and Qu, 2004; Yang et al., 2013).

The Luzon Strait transport has important impacts on the SCS circulation. The upper layer circulation in the

Foundation item: The National Natural Science Foundation of China under contract No. 42076003.
*Corresponding author, E-mail: yuwang@nmemc.org.cn

SCS is mainly driven by the SCS monsoon (Yang et al., 2002; Xue et al., 2004; Gan et al., 2006), but the Kuroshio intrusion through the Luzon Strait and mesoscale eddies that shed from Kuroshio near the Luzon Strait impose an important influence on the circulation pattern in the northern SCS (Xue et al., 2004; Nan et al., 2011, 2015; Zhang et al., 2017). In the meantime, the Luzon Strait upper layer inflow can enhance upper layer cyclonic circulation in the SCS (Chen and Xue, 2014; Xu and Oey, 2014; Li et al., 2019). The major feature of the SCS intermediate layer circulation is anticyclonic (Yuan, 2002; Shu et al., 2014; Xu and Oey, 2014), and Zhu et al. (2017) suggested that the negative potential vorticity transport caused by the Luzon Strait intermediate layer outflow is responsible for the anticyclonic circulation formation. There is a cyclonic circulation in the SCS deep layer (Qu et al., 2006; Wang et al., 2011), since the persistent deepwater overflow through the Luzon Strait provides a positive potential vorticity transport for the deep SCS and makes water move cyclonically (Lan et al., 2013). The Luzon Strait transport influences the SCS water properties (Qu et al., 2000; Wei et al., 2016) and balances the heat and salt budgets of the SCS (Qu et al., 2004; Yu et al., 2008; Fang et al., 2009). It contributes to extreme subsurface warm events in the SCS (Xiao et al., 2018) and plays an important role in long-term variabilities of salinity in the surface and subsurface layers (Zeng et al., 2016, 2021).

The shallow meridional overturning circulation (SMOC) in the upper SCS is clockwise on annual mean (Shu et al., 2014; Zhang et al., 2016), and it is essential for the vertical link between the surface layer and the subsurface layer. The SMOC has a prominent seasonal variation, with a clockwise structure in winter and an anticlockwise structure in summer (Jiang et al., 2023). The structure of the SMOC is shown by stream functions, and stream functions are under the influences of the Luzon Strait transport (Wang et al., 2004). Hence, the Luzon Strait transport may have an important influence on the SMOC. Some studies paid attention to the connection between the Luzon Strait transport and the SMOC in the SCS. Numerical experiments are carried out with the Luzon Strait open and closed in Wang et al. (2004), and their results suggested that the impact extent of the Luzon Strait transport on the upper layer stream function can reach 10°N. The SMOC can still be formed in the numerical experiment with the Luzon Strait closed, indicating that the SMOC formation is not dominated by the Luzon Strait transport. Shu et al. (2014) calculated the Lagrangian stream function to illustrate the contribution of Luzon Strait transport to the SMOC. In their results, the Lagrangian stream functions which show the SMOC structure are mainly caused by the Luzon Strait transport, suggesting that the Luzon Strait transport dominates the SMOC formation. Wang et al. (2004) and Shu et al. (2014) both pointed out that the Luzon Strait transport has an influence on the SMOC in the SCS, but they have differences on the issue whether the Luzon Strait transport dominates the SMOC formation. So far, this issue remains a matter of controversy, and there are no other studies discussing it.

In the present study, the aim is to investigate whether the Luzon Strait transport dominates the SMOC formation. The Helmholtz decomposition has been applied into the Indian Ocean to separate the Indonesian Throughflow (ITF) and the Antarctic Circumpolar Current (ACC) from the total zonally integrated flow (Han and Huang, 2020), and we apply this method into the SCS. The rest of the study is structured as follows. The data and Helmholtz decomposition method are introduced in Section 2. The Helmholtz decomposition results in winter (December) and summer (June) are presented in Section 3. Section 4 is some discussion based on numerical experiments. The summary of this study is given in Section 5.

2 Data and method

The ocean general circulation model for the earth simulator (OFES) products from 1985 to 2005 are used in this study. The OFES is based on the Modular Ocean Model (MOM3) and developed at Geophysical Fluid Dynamics Laboratory/National Oceanic and Atmospheric Administration (GFDL/NOAA). OFES has a computational domain ranging from 75°S to 75°N. Its horizontal resolution is 0.1°, and there are 54 levels in vertical direction. The vertical mixing is calculated by the K-Profile Parameterization scheme. Monthly mean wind stresses that used for the climatological seasonal integration are from the National Centers for Environmental Prediction/National Center for Atmospheric Research (NCEP/NCAR) reanalysis data. More information of OFES is available in Masumoto et al. (2004) and Sasaki et al. (2008).

The Helmholtz decomposition is used to separate the motion caused by the Luzon Strait transport from total zonally integrated flow in the SCS. According to Han and Huang (2020), zonally integrating the continuity equation leads to

$$\frac{\partial V}{\partial y}+\frac{\partial W}{\partial z}=u_{\mathrm{w}}-u_{\mathrm{e}}, \tag{1}$$

where

$$V=\int_{x_{\mathrm{w}}}^{x_{\mathrm{e}}} v\mathrm{d}x,\ W=\int_{x_{\mathrm{w}}}^{x_{\mathrm{e}}} w\mathrm{d}x, \tag{2}$$

in which V and W denote the total zonally integrated meridional velocity and vertical velocity, respectively. u_{e} and u_{w} are the zonal velocities at the eastern and western boundaries of the SCS, x_{e} and x_{w} are the eastern and western boundaries of the SCS basin, and v and w are the meridional and vertical velocity components. The right term in Eq. (1) is the divergence term. The western boundary of the SCS is the Asian landmass, and the divergence term is caused by the zonal velocities in straits at the eastern boundary. Water enters the SCS in the south-

ern part of the Luzon Strait and leaves the SCS in the northern part (Fig. 1). Water also flows out of the SCS through the Mindoro Strait near 13°N (Fig. 1; Fang et al., 2009; Yaremchuk et al., 2009). The water exchange through the Balabac Strait near 8°N is weak. The Luzon Strait transport makes the largest contribution to the nonzero divergence term.

In the Helmholtz decomposition, V and W are decomposed as

$$V = V_\Psi + V_\Phi,\ W = W_\Psi + W_\Phi, \tag{3}$$

where V_Ψ and W_Ψ are the rotational components of V and W, and V_Φ and W_Φ are the divergent components. Definitions of the rotational components and the divergent components are

$$V_\Psi = -\frac{\partial \Psi}{\partial z},\ V_\Phi = \frac{\partial \Phi}{\partial y}, \tag{4}$$

$$W_\Psi = \frac{\partial \Psi}{\partial y},\ W_\Phi = \frac{\partial \Phi}{\partial z}, \tag{5}$$

where Ψ denotes the stream function, and Φ denotes the potential function. Substituting Eqs (3)–(5) into Eq. (1) leads to a Poisson equation,

$$\frac{\partial^2 \Phi}{\partial y^2} + \frac{\partial^2 \Phi}{\partial z^2} = u_\mathrm{w} - u_\mathrm{e}. \tag{6}$$

According to Eq. (6), the divergence term is indicated by the potential function Φ. Hence, solving the Poisson equation can obtain the potential function and divergent components, and then separate the motion in the SCS caused by the Luzon Strait transport.

Boundary conditions are given to solve the Poisson equation. Following Han and Huang (2020), the normal velocity caused by the potential function Φ at the bottom boundary is zero, which leads to the bottom boundary condition

$$\frac{\partial \Phi}{\partial n} = 0, \text{ at sea bottom}, \tag{7}$$

where n is the normal unit vector at sea bottom. For the OFES products, in winter, the outward transports through the Taiwan, Mindoro, Balabac and Karimata Straits are 0.77×10^6 m^3/s, 2.98×10^6 m^3/s, 0.60×10^6 m^3/s, and 2.56×10^6 m^3/s, respectively. The outward transports, amounting to 6.91×10^6 m^3/s, are basically balanced by the inward transport of 6.87×10^6 m^3/s through the Luzon Strait with a residual of 0.04×10^6 m^3/s. In summer, the outward transports through the Taiwan, Mindoro and Balabac Straits are 1.78×10^6 m^3/s, 0.96×10^6 m^3/s, and 0.13×10^6 m^3/s, respectively. The inward transports through the Luzon and Karimata Straits are 2.18×10^6 m^3/s and 0.69×10^6 m^3/s. The outward transports (2.87×10^6 m^3/s) are balanced by the inward transports (2.87×10^6 m^3/s). Thus, the neglection of the volume flux at the sea surface is an acceptable approximation, and the surface boundary condition is taken as

$$\frac{\partial \Phi}{\partial z} = 0, \text{ at sea surface}. \tag{8}$$

The Poisson equation [Eq. (6)] is solved numerically using the "successive over-relaxation iteration" (SOR) method incorporating the surface and bottom boundary conditions [Eqs (7) and (8)]. More information of the SOR method is available in Han and Huang (2020). The Karimata Strait and the Taiwan Strait are located at the southern and northern boundaries of the SCS, respectively. The two straits are important for the mass balance of the SCS although their depths are shallow. In this study, the two straits are open in the process of solving the Poisson equation, and the flows caused by the potential function can enter or leave the SCS through them.

Two numerical experiments used in this study are designed on the basis of the Hybrid Coordinate Ocean Model (HYCOM) (Bleck, 2002). The HYCOM has been used to explore the SCS circulation (Lan et al., 2013; Zhao et al., 2020), and their results have illustrated the reliability of the HYCOM in simulating the SCS circulation. The model domain is from 78°S to 66°N with a horizontal resolution of 0.5° × 0.5°cosθ (θ denotes latitude), and there are 33 levels in the vertical direction. The ETOPO5 is used to construct the model bottom topography. The surface forcings are from the monthly NCEP/NCAR reanalysis data, including wind forcing, the net shortwave and longwave radiation, precipitation, air relative humidity, and air temperature fields. The model is integrated for 50 years with zero initial velocities and with temperature and salinity from Levitus annual mean climatology (Levitus, 1983). The Luzon Strait is open in the control run, and

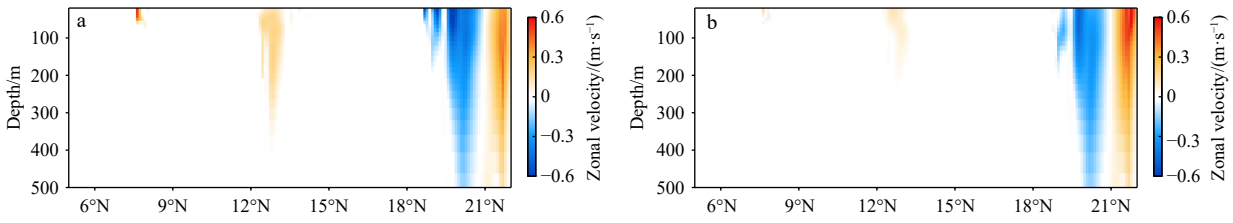

Fig. 1. Zonal velocities (m/s, eastward positive) at the eastern boundary of the SCS in winter (a) and summer (b).

closed in the sensitivity run.

3 The Helmholtz decomposition results

The curls of the decomposed divergent components and the divergences of the decomposed rotational components are basically zero, indicating the validity of our Helmholtz decomposition results. The SMOC in the SCS is depicted by the stream functions, which are calculated by vertically integrating V and V_Ψ from sea surface to sea bottom and are denoted as $\psi(V)$ and $\psi(V_\Psi)$, respectively. Along a stream function isoline, water moves clockwise around the higher value. Patterns of $\psi(V)$ and $\psi(V_\Psi)$ in winter and summer are shown in Fig. 2 to illustrate the influence of the Luzon Strait transport on the stream functions.

In winter, it is evident that the $\psi(V)$ pattern exhibits a clockwise SMOC spanning a 9°–18°N latitude range (Fig. 2a). It consists of the water sinking in the northern SCS, the water rising in the southern SCS, the northward surface transport and the southward subsurface transport. After the motion generated by the Luzon Strait transport being removed, the clockwise SMOC between 9°N and 18°N is still shown clearly in the $\psi(V_\Psi)$ pattern (Fig. 2b). The similarity between the $\psi(V)$ pattern and the $\psi(V_\Psi)$ pattern indicates that the Luzon Strait transport has no significant influence on the SMOC structure in winter.

In summer, the $\psi(V)$ pattern presents an anticlockwise SMOC in the southern SCS, with an upwelling branch near 12°N, a downwelling branch near 6°N, a southward surface branch and a northward subsurface branch (Fig. 2c). When the motion caused by the Luzon Strait transport is removed, the $\psi(V_\Psi)$ pattern closely resembles the $\psi(V)$ pattern, and an anticlockwise summer SMOC is still maintained in the southern SCS (Fig. 2d). Hence, the Luzon Strait transport imparts little influence on the SMOC structure in summer.

The divergent component V_Φ that separated from total zonally integrated meridional velocity is shown in Fig. 3, reflecting features of the motion that caused by the Luzon Strait transport. The Luzon Strait transport is inward to the SCS from the Pacific Ocean and the Mindoro Strait (near 13°N, south of the Luzon Strait) transport is outward to the Sulu Sea (Fang et al., 2009; Yaremchuk et al., 2009), and thus, the divergent component V_Φ in the upper 100 m depicts a distinct southward flow extending from 20°N to 13°N (Fig. 3). This southward flow has higher intensity in winter and lower intensity in summer, also corresponding to the prominent seasonal variation of the Luzon Strait upper layer transport which is stronger in winter and weaker in summer (Qu, 2000; Zhang et al., 2015). This southward flow makes differences between the $\psi(V)$ pattern and the $\psi(V_\Psi)$ pattern north of 13°N more significant in winter (Fig. 2). The Luzon Strait transport also causes flows south of 13°N, but intensities of these flows are weaker than that north of 13°N (Fig. 3). As a result, differences between the $\psi(V)$ pattern and the $\psi(V_\Psi)$ pattern south of 13°N are less obvious than that north of 13°N (Fig. 2). In general, the Helmholtz decomposition results suggest that the Luzon Strait transport does not dominate the formation and seasonal variation of the SMOC although it imposes some influence on the upper layer stream functions, which is consistent with the results in Wang et al. (2004).

4 Discussion

Two numerical experiments are conducted to further confirm the conclusion in Section 3. The Luzon Strait is open in the control run and closed in the sensitivity run. The two numerical experiments in this study use the SCS topography and keep the Taiwan, Mindoro, and Karimata Straits open. Our numerical experiments are improved when compared with the numerical experiments in Wang et al. (2004) which have a flat bottom (1 000 m) and treat most straits as an enclose boundary excluding the Luzon

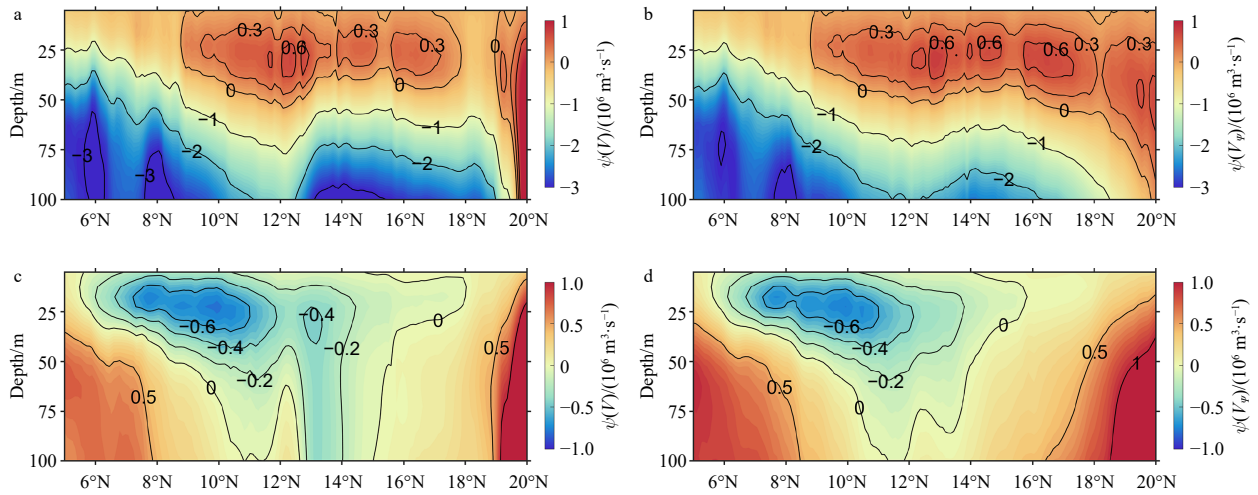

Fig. 2. Stream functions (10^6 m^3/s) obtained by vertically integrating the total zonally integrated meridional velocity V (a) and the rotational component V_Ψ (b) in winter. c and d are same as a and b, but in summer.

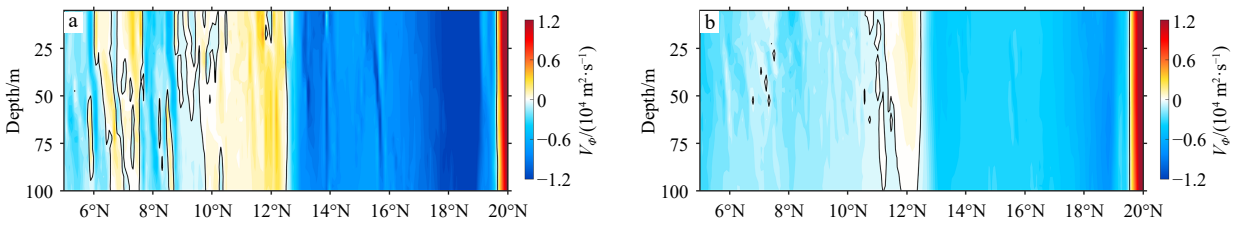

Fig. 3. The divergent component V_Φ (10^4 m^2/s, northward positive) of total zonally integrated meridional velocity in winter (a) and summer (b).

Strait.

We validate the surface circulations from the control run using the horizontal velocities of Ocean Surface Currents Analyses Real-time version 2.0 (OSCARv2.0) products from 1993 to 2020 which are calculated from sea surface height, surface wind and sea surface temperature that collected from satellites and *in situ* measurements (Bonjean and Lagerloef, 2002). The surface circulations from control run and OSCARv2.0 products are shown in Fig. 4. In winter, water enters into the SCS through the Luzon Strait, and there is a basin scale cyclonic gyre in the SCS (Figs 4a and c). In summer, the Kuroshio leaps across the Luzon Strait, and an anticyclonic gyre occurs in the southern SCS (Figs 4b and d). The surface circulation patterns near the Luzon Strait and within the SCS from the control run results are consistent with those from observations. Besides, in the control run result, the Luzon Strait transport above 100 m is westward in winter with a strength of 2.45 × 10^6 m^3/s, while it is eastward in summer with a strength of 1.46 × 10^6 m^3/s, which is consistent with previous studies (Fang et al., 2009; Zhu et al., 2016). Overall, the control run is capable of simulating the Luzon Strait transport and the SCS circulations.

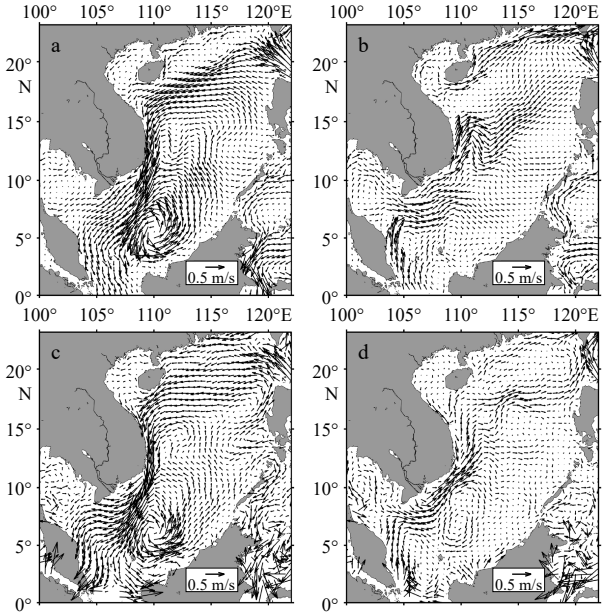

Fig. 4. Surface circulation (in m/s) in winter (a) and summer (b) from the control run. c and d are same as a and b, but from OSCARv2.0 products.

Stream functions of two numerical experiments are presented in Fig. 5. In the control run, the winter pattern shows a northern cell located between 14°N and 19°N and a southern cell located between 7°N and 10°N. This forms a clockwise SMOC in winter, with the 7°–19°N latitude range and 50 m depth (Fig. 5a). The summer pattern exhibits an anticlockwise SMOC above 30 m between 6°N and 10°N, confined to the southern SCS (Fig. 5b). These results suggest that the existence of SMOC and its seasonal variation are well reproduced in the control run.

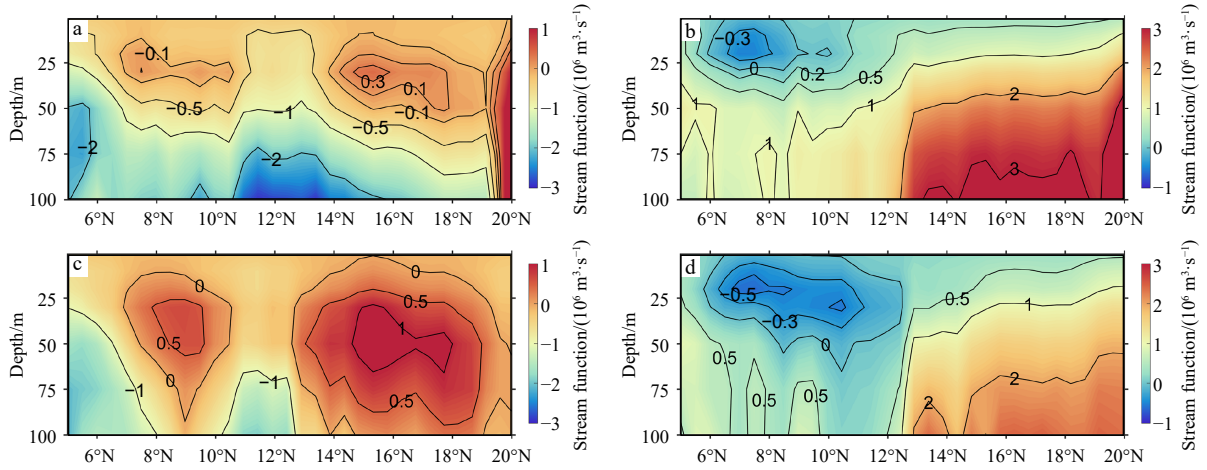

Fig. 5. SMOC stream functions (10^6 m^3/s) in winter (a) and summer (b) from the control run. c and d are same as a and b, but from the sensitivity run.

In the sensitivity run, the winter SMOC remains clockwise and occupies the upper layer, with two clockwise cells (Fig. 5c). It spans a 7°–19°N latitude range and reaches a depth of more than 100 m. The summer SMOC still keeps anticlockwise and is also confined to the southern SCS (Fig. 5d). It is presented between 6°N and 12°N and extends to a depth of around 50 m. The results in the sensitivity run are similar to those in the control run. Thus, although the Luzon strait is closed, the SMOC structure and its seasonal variation still exist.

The numerical experiments also suggest that the physical processes within the SCS, instead of the Luzon Strait transport, dominate the formation and seasonal variation of the SCS SMOC. The SMOC formation processes have been analyzed in Jiang et al. (2023), and the SCS monsoon is the primary driving factor for the SMOC. In winter, the northeasterly monsoon causes strong wind stirring and buoyancy loss, leading to the mixed layer deepening and thermocline outcropping in the northern SCS, which provides conditions for the subduction occurrence. The water, subducted by Ekman pumping, conserves potential vorticity and moves southward. The subducted water rises to the sea surface along the sloping thermocline in the southern SCS, and is pushed back to the northern SCS by the northward Ekman transport. Thus, the clockwise winter SMOC is formed. In summer, the southwesterly monsoon generates upwelling and downwelling in the regions east of Vietnam and northwest of the Kalimantan Island, respectively. The southward Ekman transport and the northward western boundary current connect the two regions and close the anticlockwise summer SMOC.

5 Summary

This study focuses on the issue whether the SMOC formation and its seasonal variation are dominated by the Luzon Strait transport. To address the issue, the Helmholtz decomposition is applied based on OFES products. Results show that the motion caused by the Luzon Strait transport is characterized as a distinct southward flow between 13°N and 20°N. Although this motion has some influence on the structure of stream function in the upper layer, the clockwise winter SMOC and the anticlockwise summer SMOC can still exist significantly after it being removed. The SMOC formation and its seasonal variation are dominated by the physical processes within the SCS instead of the Luzon Strait transport. Further, this conclusion can be confirmed based on the numerical experiments, which show that the SMOC structure and its seasonal variation can still be reproduced with closed Luzon Strait.

The SCS monsoon is the primary driving factor for the SMOC (Jiang et al., 2023). The formation of clockwise winter SMOC is related to the subduction in the northern SCS, and the formation of anticlockwise summer SMOC is related to the Ekman suction and Ekman pumping in the southern SCS. But the Luzon Strait transport also has an influence on the SMOC, which has been pointed out by previous studies (Wang et al., 2004; Shu et al., 2014) and can be seen from the differences between $\psi(V)$ and $\psi(V_\Psi)$ patterns and the differences between two numerical experiments results. The related physical processes of the Luzon Strait transport impacting the SMOC are worthy of further study.

Acknowledgements

We are grateful to the Asia-Pacific Data-Research Center at the University of Hawaii for the data support. The OFES products are obtained from http://apdrc.soest.hawaii.edu/datadoc/ofes/ofes.php. The OSCARv2.0 products are available from https://www.esr.org/research/oscar/overview/. We thank Han Lei for sharing the Matlab code of Helmholtz decomposition (https://github.com/leihan-SDU/IMOC/). We also thank the two anonymous reviewers for their valuable comments which improve the earlier version of this paper.

References

Bleck R. 2002. An oceanic general circulation model framed in hybrid isopycnic-Cartesian coordinates. Ocean Modelling, 4(1): 55–88, doi: 10.1016/S1463-5003(01)00012-9

Bonjean F, Lagerloef G S E. 2002. Diagnostic model and analysis of the surface currents in the tropical Pacific Ocean. Journal of Physical Oceanography, 32(10): 2938–2954, doi: 10.1175/1520-0485(2002)032<2938:DMAAOT>2.0.CO;2

Chen Gengxin, Xue Huijie. 2014. Westward intensification in marginal seas. Ocean Dynamics, 64(3): 337–345, doi: 10.1007/s10236-014-0691-z

Chu P C, Li Rongfeng. 2000. South China Sea isopycnal-surface circulation. Journal of Physical Oceanography, 30(9): 2419–2438, doi: 10.1175/1520-0485(2000)030<2419:SCSISC>2.0.CO;2

Deng Hengxiang, Huang Peng, Tanhua T, et al. 2018. Observations of the intermediate water exchange between the South China Sea and the Pacific Ocean deduced from transient tracer measurements. Journal of Geophysical Research: Oceans, 123(10): 7495–7510, doi: 10.1029/2018JC014103

Fang Guohong, Susanto D, Soesilo I, et al. 2005. A note on the South China Sea shallow interocean circulation. Advances in Atmospheric Sciences, 22(6): 946–954, doi: 10.1007/BF02918693

Fang Guohong, Wang Yonggang, Wei Zexun, et al. 2009. Interocean circulation and heat and freshwater budgets of the South China Sea based on a numerical model. Dynamics of Atmospheres and Oceans, 47(1–3): 55–72, doi: 10.1016/j.dynatmoce.2008.09.003

Gan Jianping, Li H, Curchitser E N, et al. 2006. Modeling South

China Sea circulation: response to seasonal forcing regimes. Journal of Geophysical Research: Oceans, 111(C6): C06034, doi: 10.1029/2005JC003298

Han Lei, Huang Ruixin. 2020. Using the Helmholtz decomposition to define the Indian Ocean meridional overturning streamfunction. Journal of Physical Oceanography, 50(3): 679–694, doi: 10.1175/JPO-D-19-0218.1

Hsin Y C, Wu Chau-Ron, Chao S Y. 2012. An updated examination of the Luzon Strait transport. Journal of Geophysical Research: Oceans, 117(C3): C03022, doi: 10.1029/2011JC007714

Jiang Kun, Wang Yu, Sun Yan, et al. 2023. The seasonal variation of shallow meridional overturning circulation in the South China Sea and the related dynamics. Ocean Modelling, 186: 102242, doi: 10.1016/j.ocemod.2023.102242

Lan Jian, Zhang Ningning, Wang Yu. 2013. On the dynamics of the South China Sea deep circulation. Journal of Geophysical Research: Oceans, 118(3): 1206–1210, doi: 10.1002/jgrc.20104

Levitus S. 1983. Climatological atlas of the world ocean. Eos, Transactions American Geophysical Union, 64(49): 962–963, doi: 10.1029/EO064i049p00962-02

Li Mingting, Wei Jun, Wang Dongxiao, et al. 2019. Exploring the importance of the Mindoro-Sibutu pathway to the upper-layer circulation of the South China Sea and the Indonesian Throughflow. Journal of Geophysical Research: Oceans, 124(7): 5054–5066, doi: 10.1029/2018JC014910

Masumoto Y, Sasaki H, Kagimoto T, et al. 2004. A fifty-year eddy-resolving simulation of the world ocean: preliminary outcomes of OFES (OGCM for the Earth Simulator). Journal of the Earth Simulator, 1: 35–56

Metzger E J, Hurlburt H E. 1996. Coupled dynamics of the South China Sea, the Sulu Sea, and the Pacific Ocean. Journal of Geophysical Research: Oceans, 101(C5): 12331–12352, doi: 10.1029/95JC03861

Nan Feng, Xue Huijie, Xiu Peng, et al. 2011. Oceanic eddy formation and propagation southwest of Taiwan. Journal of Geophysical Research, 116(C12): C12045, doi: 10.1029/2011JC007386

Nan Feng, Xue Huijie, Yu Fei. 2015. Kuroshio intrusion into the South China Sea: a review. Progress in Oceanography, 137: 314–333, doi: 10.1016/j.pocean.2014.05.012

Qu Tangdong. 2000. Upper-layer circulation in the South China Sea. Journal of Physical Oceanography, 30(6): 1450–1460, doi: 10.1175/1520-0485(2000)030<1450:ULCITS>2.0.CO;2

Qu Tangdong. 2002. Evidence for water exchange between the South China Sea and the Pacific Ocean through the Luzon Strait. Acta Oceanologica Sinica, 21(2): 175–185

Qu Tangdong, Girton J B, Whitehead J A. 2006. Deepwater overflow through Luzon Strait. Journal of Geophysical Research: Oceans, 111(C1): C01002, doi: 10.1029/2005JC003139

Qu Tangdong, Kim Y Y, Yaremchuk M, et al. 2004. Can Luzon Strait transport play a role in conveying the impact of ENSO to the South China Sea?. Journal of Climate, 17(18): 3644–3657, doi: 10.1175/1520-0442(2004)017<3644:CLSTPA>2.0.CO;2

Qu Tangdong, Mitsudera H, Yamagata T. 2000. Intrusion of the North Pacific waters into the South China Sea. Journal of Geophysical Research: Oceans, 105(C3): 6415–6424, doi: 10.1029/1999JC900323

Sasaki H, Nonaka M, Masumoto Y, et al. 2008. An eddy-resolving hindcast simulation of the quasiglobal ocean from 1950 to 2003 on the Earth Simulator. In: Hamilton K, Ohfuchi W, eds. High Resolution Numerical Modelling of the Atmosphere and Ocean. New York: Springer, 157–185, doi: 10.1007/978-0-387-49791-4_10

Shu Yeqiang, Xue Huijie, Wang Dongxiao, et al. 2014. Meridional overturning circulation in the South China Sea envisioned from the high-resolution global reanalysis data GLBa0.08. Journal of Geophysical Research: Oceans, 119(5): 3012–3028, doi: 10.1002/2013JC009583

Tian Jiwei, Yang Qingxuan, Liang Xinfeng, et al. 2006. Observation of Luzon Strait transport. Geophysical Research Letters, 33(19): L19607, doi: 10.1029/2006GL026272

Wang Dongxiao, Liu Xiongbin, Wang Wenzhi, et al. 2004. Simulation of meridional overturning in the upper layer of the South China Sea with an idealized bottom topography. Chinese Science Bulletin, 49(7): 740–746, doi: 10.1007/BF03184275

Wang Guihua, Xie Shangping, Qu Tangdong, et al. 2011. Deep South China Sea circulation. Geophysical Research Letters, 38(5): L05601, doi: 10.1029/2010GL046626

Wei Jun, Malanotte-Rizzoli P, Li Mingting, et al. 2016. Decomposition of thermal and dynamic changes in the South China Sea induced by boundary forcing and surface fluxes during 1970–2000. Journal of Geophysical Research: Oceans, 121(11): 7953–7972, doi: 10.1002/2016JC012078

Wu Junhui, Lao Qibin, Chen Fajin, et al. 2021. Water mass processes between the South China Sea and the Western Pacific through the Luzon Strait: insights from hydrogen and oxygen isotopes. Journal of Geophysical Research: Oceans, 126(8): e2021JC017484, doi: 10.1029/2021JC017484

Xiao Fuan, Zeng Lili, Liu Qinyan, et al. 2018. Extreme subsurface warm events in the South China Sea during 1998/99 and 2006/07: observations and mechanisms. Climate Dynamics, 50(1): 115–128, doi: 10.1007/s00382-017-3588-y

Xu Fanghua, Oey Lie-Yauw. 2014. State analysis using the Local Ensemble Transform Kalman Filter (LETKF) and the three-layer circulation structure of the Luzon Strait and the South China Sea. Ocean Dynamics, 64(6): 905–923, doi: 10.1007/s10236-014-0720-y

Xue Huijie, Chai Fei, Pettigrew N, et al. 2004. Kuroshio intrusion and the circulation in the South China Sea. Journal of Geophysical Research: Oceans, 109(C2): C02017, doi: 10.1029/2002JC001724

Yang Jiayan, Lin Xiaopei, Wu Dexing. 2013. On the dynamics of the seasonal variation in the South China Sea throughflow transport. Journal of Geophysical Research: Oceans, 118(12): 6854–6866, doi: 10.1002/2013JC009367

Yang Haijun, Liu Qingyu, Liu Zhengyu, et al. 2002. A general

circulation model study of the dynamics of the upper ocean circulation of the South China Sea. Journal of Geophysical Research: Oceans, 107(C7): 3085, doi: 10.1029/2001JC001084

Yaremchuk M, McCreary J, Yu Zuojun, et al. 2009. The South China Sea throughflow retrieved from climatological data. Journal of Physical Oceanography, 39(3): 753–767, doi: 10.1175/2008JPO3955.1

Yaremchuk M, Qu Tangdong. 2004. Seasonal variability of the large-scale currents near the coast of the Philippines. Journal of Physical Oceanography, 34(4): 844–855, doi: 10.1175/1520-0485(2004)034<0844:SVOTLC>2.0.CO;2

Yu Zuojun, McCreary J P, Yaremchuk M, et al. 2008. Subsurface salinity balance in the South China Sea. Journal of Physical Oceanography, 38(2): 527–539, doi: 10.1175/2007JPO3661.1

Yuan Dongliang. 2002. A numerical study of the South China Sea deep circulation and its relation to the Luzon Strait transport. Acta Oceanologica Sinica, 21(2): 187–202

Zeng Lili, Chassignet E P, Xu Xiaobiao, et al. 2021. Multi-decadal changes in the South China Sea mixed layer salinity. Climate Dynamics, 57(1): 435–449, doi: 10.1007/s00382-021-05711-1

Zeng Lili, Wang Dongxiao, Xiu Peng, et al. 2016. Decadal variation and trends in subsurface salinity from 1960 to 2012 in the northern South China Sea. Geophysical Research Letters, 43(23): 12181–12189, doi: 10.1002/2016GL071439

Zhang Ningning, Lan Jian, Ma Jie, et al. 2016. The shallow meridional overturning circulation in the South China Sea and the related internal water movement. Acta Oceanologica Sinica, 35(7): 1–7, doi: 10.1007/s13131-016-0900-3

Zhang Zhiwei, Zhao Wei, Tian Jiwei, et al. 2015. Spatial structure and temporal variability of the zonal flow in the Luzon Strait. Journal of Geophysical Research: Oceans, 120(2): 759–776, doi: 10.1002/2014JC010308

Zhang Zhiwei, Zhao Wei, Qiu Bo, et al. 2017. Anticyclonic eddy sheddings from Kuroshio loop and the accompanying cyclonic eddy in the northeastern South China Sea. Journal of Physical Oceanography, 47(6): 1243–1259, doi: 10.1175/JPO-D-16-0185.1

Zhao Wei, Hou Yijun, Qi Peng, et al. 2009. The effects of monsoons and connectivity of South China Sea on the seasonal variations of water exchange in the Luzon Strait. Journal of Hydrodynamics, 21(2): 264–270, doi: 10.1016/S1001-6058(08)60144-4

Zhao Xiao, Zhou Chun, Xu Xiaobiao, et al. 2020. Deep circulation in the South China Sea simulated in a regional model. Ocean Dynamics, 70(11): 1461–1473, doi: 10.1007/s10236-020-01411-2

Zhu Yaohua, Fang Guohong, Wei Zexun, et al. 2016. Seasonal variability of the meridional overturning circulation in the South China Sea and its connection with inter-ocean transport based on SODA2.2.4. Journal of Geophysical Research: Oceans, 121(5): 3090–3105, doi: 10.1002/2015JC011443

Zhu Yaohua, Sun Junchuan, Wang Yonggang, et al. 2017. Effect of potential vorticity flux on the circulation in the South China Sea. Journal of Geophysical Research: Oceans, 122(8): 6454–6469, doi: 10.1002/2016JC012375